Large-Scale Structure in Gels of Attractive Block Copolymer Micelles†

Mark A. Crichton‡ and Surita R. Bhatia*

Department of Chemical Engineering, University of Massachusetts Amherst, 686 North Pleasant Street, Amherst, Massachusetts 01003

Received March 31, 2005. In Final Form: August 6, 2005

We have used ultra-small-angle scattering (USANS) and fluorescence microscopy to demonstrate the existence of a nonfractal large-scale structure in attractive micellar gels of poly(styrene)−poly(acrylic acid) block copolymers, which have some characteristics of attractive colloidal glasses. The nature of the large-scale structure appears to depend systematically on the strength of attraction. Our systems display scattering that follows $I \sim q^x$ in the low q regime, with x varying from approximately −3 to −4 as the strength of attraction is decreased. This scattering behavior appears to be the result of surface scattering from large, highly polydisperse aggregates with rough interfaces.

Introduction

Arrested states of soft matter, such as colloidal glasses and fractal colloidal gels, are interesting from both a fundamental point of view and in applications such as emulsions, foams, cosmetics, and foods. Here, our use of the terms "gel" and "glass" are consistent with the descriptions given by Bonn and co-workers[1] and Pham et al.[2] In colloidal gels, attractive forces impart a percolated network structure, which gives rise to an elastic response. The particle localization length is controlled by the range of the interparticle attraction. Colloidal glasses can be either repulsion-driven or attraction-driven.[2] In the former case, repulsive interparticle forces are dominant, and structural arrest occurs through caging of particles by their neighbors. Introducing weak short-range attractions to such a system melts the glass; however, as the strength of attraction is increased, a new type of glassy state is formed. In this attraction-driven glass, long-lived interparticle bonds form and are responsible for structural arrest.[2] In this case, the strength of attraction is typically far weaker than those present in attractive colloidal gels.

Colloidal gels and glasses can exhibit similar rheological properties, making them difficult to distinguish experimentally; however, some authors have suggested that they may be distinguished by structural differences.[1] Several colloidal gels exhibit a mass fractal structure, where the fractal dimension can be probed via low q scattering.[3] For such systems, the scattered intensity scales as $I \sim q^{-df}$ in the low q regime, with typical values for the fractal dimension d_f in the range 1.8−2.2, depending upon the mechanism for aggregation.[3,4] However, dense colloidal gels can also exhibit low q scattering with exponents between −3 and −4, characteristic of surface scattering. A series of papers by the Schweizer and Zukoski groups[5−7] utilize USAXS to examine the microstructure of hard-sphere colloidal silica with a polymer-induced depletion attraction. Their data show a power law dependence of $I \sim q^{-3.5}$ in the low q range, which they interpret as the formation of dense, polydisperse aggregates with fractally rough surfaces. A length scale of 0.5−1.0 μm was found for the aggregate size, corresponding to 5−8 particle diameters. Neither the aggregate size nor low-q exponent was found to depend systematically on polymer concentration.[6,7]

There is some expectation that colloidal glasses exhibit no large-scale structure,[1] although this has not been shown theoretically to our knowledge. Correspondingly, the structure factor $S(q)$ should have no characteristic features at low q. This has been verified experimentally for several repulsion-driven colloidal glasses; for example, light scattering[1,8,9] and USANS[10] on isotropic repulsive glasses of Laponite, a colloidal clay, show no q-dependence of $S(q)$ in the low q regime. However, there have been few studies on the large-scale structure of attractive glasses. Pontoni and Narayanan[11] performed ultra-small-angle X-ray scattering (USAXS) on an attractive glass of colloidal silica in a mixed solvent of 2,6-lutidine and D_2O. These particles exhibit a short-range attraction that increases as temperature increases. Below the glass transition, no low-q excess scattering is observed, whereas above the glass transition, $I \sim q^{-4}$ in the low q regime. Fits to their USAXS spectra suggest large clusters with sizes of 8−10 μm.

Here, we probe the large-scale structure of poly(styrene)−poly(acrylic acid/ethyl acrylate) block copolymers (PS−PAA/EA), which form spherical micelles in water that associate via the hydrophobic EA groups (Figure 1). We have shown previously that these micelles form viscoelastic solids that have some characteristics of attractive colloidal glasses,[12] where the strength of attraction is inversely related to the degree of hydrolysis of

† Part of the Bob Rowell Festschrift special issue.

* Corresponding author. E-mail: sbhatia@ecs.umass.edu.

‡ Current address: Infineum, Linden, NJ 07036.

(1) Tanaka, H.; Meunier, J.; Bonn, D. *Phys. Rev. E* **2004**, *69*, 031404.

(2) Pham, K. N.; Puertas, A. M.; Bergenholtz, J.; Egelhaaf, S. U.; Moussaid, A.; Pusey, P.; Schofield, A. B.; Cates, M. E.; Fuchs, M.; Poon, W. C. K. *Science* **2002**, *296*, 104−106.

(3) Schaefer, D. W.; Martin, J. E.; Wiltzius, P.; Cannell, D. S. *Phys. Rev. Lett.* **1984**, *52*, 2371−2374.

(4) Dimon, P.; Sinha, S. K.; Weitz, D. A.; Safinya, C. R.; Smith, G. S.; Varady, W. A.; Lindsay, H. M. *Phys. Rev. Lett.* **1986**, *57*, 595−598.

(5) Ramakrishnan, S.; Chen, Y. L.; Schweizer, K. S.; Zukoski, C. F. *Phys. Rev. E* **2004**, *70*, 040401.

(6) Shah, S. A.; Chen, Y. L.; Ramakrishnan, S.; Schweizer, K. S.; Zukoski, C. F. *J. Phys.: Condens. Matter.* **2003**, *15*, 4751−4778.

(7) Shah, S. A.; Chen, Y. L.; Schweizer, K. S.; Zukoski, C. F. *J. Chem. Phys.* **2003**, *119*, 8747−8760.

(8) Knaebel, A.; Bellour, M.; Munch, J. P.; Viasnoff, V.; Lequeux, F.; Harden, J. L. *Europhys. Lett.* **2000**, *52*, 73−79.

(9) Bonn, D.; Kellay, H.; Tanaka, H.; Wegdam, G.; Meunier, J. *Langmuir* **1999**, *15*, 7534−7536.

(10) Bhatia, S.; Barker, J.; Mourchid, A. *Langmuir* **2003**, *19*, 532−535.

(11) Pontoni, D.; Narayanan, T. *J. Appl. Crystallogr.* **2003**, *36*, 787−790.

(12) Bhatia, S. R.; Mourchid, A. *Langmuir* **2002**, *18*, 6469−6472.

10.1021/la0508487 CCC: $30.25
Published on Web 09/17/2005

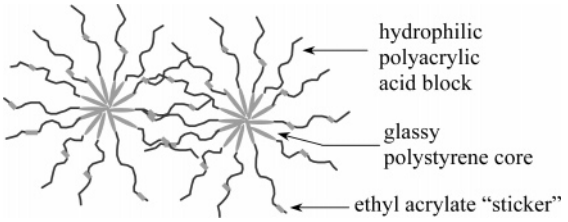

Figure 1. PS−PAA/EA micelles associated via ethyl acrylate (EA) stickers.

the PAA/EA block, f.[13] Recent dynamic light scattering and rheological studies[13] demonstrate that these micelles undergo a re-entrant glass transition, as predicted by mode-coupling theory.[2]

It is important to note the differences between our system and previously studied hard sphere colloids. We perform all our experiments at pH 10; at this high pH, we expect all acrylic acid groups to be charged. However, because counterions are trapped in the corona brush, the micelles have a softer repulsion than might be expected and allow for a great deal of compression and/or interpenetration of the corona chains. This is consistent with other scattering studies of block polyelectrolyte micelles.[15,16] Furthermore, the range of attraction in our system is quite difficult to quantify and control, unlike hard-sphere colloids with polymer-induced depletion attractions. Thus, it is unclear whether our results can truly be interpreted in terms of existing theories for attractive colloids, and whether they will be extensible to hard sphere colloids.

Experimental Details

The diblock polymers were supplied by Rhodia Inc. as polystyrene-poly(ethyl acrylate). The molecular weight of the polystyrene−poly(ethyl acrylate) material was 2000 g/mol of polystyrene and 19468 g/mol of poly(ethyl acrylate). The polymer was supplied as an aqueous suspension of latex particles of approximately 40 wt %. The hydrolysis reaction was run with 10 wt % polymer in water at 363 K. When the polymer solution reached 363 K, a 2 M NaOH aqueous solution was added dropwise. The amount of NaOH added was dependent on the desired degree of hydrolysis. The reaction mixture was then held at 363 K for 24 h. The final degree of hydrolysis was determined using a 200 MHz ^{1}H NMR instrument. After hydrolysis, the polymer was dialyzed using regenerated cellulose membranes with a molecular weight cutoff of 6000−8000 (SpectraPor 1, Spectrum Laboratories) against an aqueous NaOH solution at pH 10 for about one week. This was done to remove impurities and normalize the charge density along the polymer backbone.

SANS data were recorded on the 30-m small-angle instrument NG3 at the NIST Center for Neutron Research (NCNR), and USANS experiments were performed on NCNR's perfect crystal SANS instrument, BT5. Samples for USANS and SANS were prepared by dissolving freeze-dried polymer in D_2O (Cambridge Isotope Laboratories) and stirring for several days at 353 K. Spectra were obtained at 25 °C for a polymer concentration of 4.0 wt %. Quartz sample cells with a path length of 1 mm were used. The USANS and SANS data together cover a q-range of approximately 0.00005 Å^{-1} < q < 0.3 Å^{-1} (where $q = 4\pi/\lambda \sin 2\theta$ with θ = half the scattering angle and λ = wavelength of the incident neutrons).

Fluorescence microscopy was performed on samples with a polymer concentration of 2.0 wt %. The samples were prepared by dissolving freeze-dried polymer in Nanopure water and stirring for several days at 353 K. The samples were then allowed to cool to room temperature. To the samples was added 6.1×10^{-7} of BODIPY 505/515 (Molecular Probes). The samples were then stirred to disperse the dye and stored in the dark at room temperature for 24 h to allow the gel to equilibrate. After this, a small amount was placed between a glass slide and cover slip and placed into an Olympus IX71 microscope equipped with an EGFP filter set. Fluorescence micrographs were analyzed using the ImageJ software package.

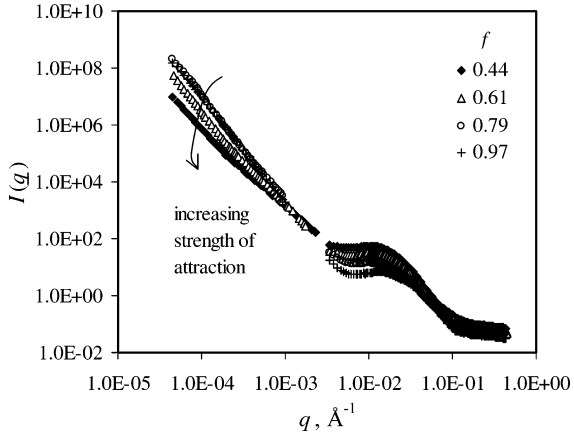

Figure 2. USANS and SANS spectra for attractive glasses of PS−PAA/EA micelles. Spectra are shown for a series with increasing strength of attraction, from weakly attractive (f = 0.97) to strongly attractive (f = 0.44).

Results and Discussion

Figure 2 shows the combined USANS and SANS spectra for a series of micellar gels with decreasing strength of attraction, from strongly attractive (f = 0.44) to weakly attractive (f = 0.97). A broad peak is observed in the SANS spectra, corresponding to intermicellar correlations. No peak is observed in the low q regime probed by USANS, as is sometimes present if large aggregates with a well-defined characteristic length scale are present.[17] Rather, we obtain a power-law dependence over a large range of q, with the scattered intensity I at low q scaling as $I \sim q^x$. This indicates a large-scale structure that persists over a range of length scales. That we observe this behavior from q = 0.001 to 0.00005 Å^{-1} indicates that the smallest aggregates are approximately 0.6 μm, whereas the largest aggregates are at least 12 μm. These correspond to approximately 30−600 micelle diameters.

To analyze these data, we extend the classical expression for $I(q)$ to include the low q regime as follows:

$$I(q) = N(\Delta\rho_b)^2 P(q) S(q) + Aq^x \qquad (1)$$

where N is the number density of micelles, $\Delta\rho_b$ is the difference in scattering length density, $P(q)$ and $S(q)$ are the form and structure factor, respectively. Added to this is the term Aq^x, which is a simple power law to fit the USANS data. A and x are fitting parameters. For the form factor, $P(q)$, we used a polydisperse sphere model. This model contains two parameters, R, which we interpret as the radius of the micelle, and σ, the width of the size distribution. For the structure factor, either an adhesive hard sphere (AHS) or hard sphere (HS) model was used to describe the interactions between micelles. The fitted parameters in this model are R_{HS}, the radius of interaction, N_{agg}, the micelle aggregation number, and τ, the stickiness parameter in the case of the AHS fits. The volume fraction

(13) Bhatia, S. R.; Mourchid, A.; Joanicot, M. *Curr. Opin. Colloid Interface Sci.* **2001**, *6*, 471−478.
(14) Grandjean, J.; Mourchid, A. *Europhys. Lett.* **2004**, *65*, 712−718.
(15) Groenewegen, W.; Egelhaaf, S. U.; Lapp, A.; van der Maarel, J. R. C. *Macromolecules* **2000**, *33*, 4080−4086.
(16) Groenewegen, W.; Lapp, A.; Egelhaaf, S. U.; van der Maarel, J. R. C. *Macromolecules* **2000**, *33*, 3283−3293.
(17) Takeshita, H.; Kanaya, T.; Nishida, K.; Kaji, K.; Takahashi, T.; Hashimoto, M. *Phys. Rev. E* **2000**, *61*, 2125−2128.

Table 1. Critical Concentrations and Effective Volume Fractions for Gel Formation, Estimated from Rheology,[13] and Parameters from SANS/USANS Data Fitting

f	c^* for gel formation (wt %)	ϕ^*_{eff}	ϕ_{eff} at 4 wt %	R (Å)	R_{HS} (Å)	σ (Å)	N_{agg}	τ	x
0.44	0.9	0.87	3.8	114.6 ± 1.0	140.4 ± 0.3	28.8 ± 1.0	208	0.015 ± 0.006	−2.90
0.61	1.0	0.98	3.9	108.1 ± 1.0	149 ± 15	27.7 ± 1.5	180	0.020 ± 0.007	−3.11
0.78	1.2	1.5	5.0	94.7 ± 1.7	96 ± 32	25.0 ± 2.4	101		−3.55
0.97	1.7	2.5	5.9	79.4 ± 1.5	79 ± 26	21.0 ± 2.0	54		−3.76

appearing the AHS and HS structure factors was determined self-consistently from N_{agg} and R_{HS} in order to minimize the number of fitting parameters; the details of this are given elsewhere.[18]

Parameters obtained from the fits are given in Table 1, along with the critical concentration for gelation determined from rheology,[13] estimated critical effective volume fraction, and effective volume fraction for the SANS/USANS samples. As discussed by Vlassopoulos and coworkers[19] there is ambiguity in determining the effective volume fraction for soft colloidal systems such as these due to compression of the particles. Additionally, one may choose the hard core radius of the particles or the hydrodynamic radius of the particles to scale the effective volume fraction. Finally, a small error in the experimentally determined radius can lead to large errors in estimating the volume fraction. In Table 1, we have scaled the effective volume fraction on the micelle radius, R, determined from SANS fits

$$\phi_{eff} = \frac{4\pi R^3 N}{3} \tag{2}$$

where N is the number density of micelles, given by

$$N = \frac{cN_{Av}}{MW_{PS-PAA}N_{agg}} \tag{3}$$

with the polymer concentration, c, and Avogadro's number, N_{Av}. Using this scaling, the concentrations required for gel formation are far above close-packed, indicating a significant amount of compression of the micelles or interpenetration of the corona chains. Samples for neutron scattering studies at 4 wt % all have effective volume fractions above unity, suggesting that these samples are highly crowded.

The micelle radii are in the range 79−114 Å and decrease with increasing f, corresponding to a decrease in the aggregation number with increasing f. This is likely due to increasing charge density of the corona with increasing f. We have discussed this trend in a previous publication,[18] and it agrees well with theoretical predictions for block polyelectrolyte micelles.[20,21] The intermicellar potential is characterized by R_{HS} and τ; unfortunately, the fits are fairly insensitive to the values of these parameters, as evidenced by the large relative uncertainty in the fit values. The values for R_{HS} decrease with increasing f, suggesting a decrease in the range of the repulsion between micelles. Systems for which no value of τ is given in Table 1 (f = 0.97 and 0.79) were well-fit with a HS structure factor, rather than the AHS structure factor, which is consistent with the idea that systems with higher f have weaker intermicellar attractions. It could be argued that, since the HS structure factor fits the data for higher f, it is not clear that there are significant attractions in these systems. However, fully hydrolyzed PS−PAA systems of similar molecular weight do not show gel formation until concentrations higher than roughly 25 wt %; in addition, dynamic light scattering on our partially hydrolyzed systems shows a population of aggregates even at very low concentrations of 0.0035 wt %.[22]

The large uncertainty in R_{HS} and τ makes it difficult to draw definitive conclusions about the effect of f on the intermicellar potential. In previous work, we have discussed the limitations of the AHS model in describing these systems.[18] It does not capture the softness of the micelles and the range of intermicellar attraction. However, although more accurate models are available to describe the structure factor of polymeric micelles, we do not believe that our spectra have enough resolution to warrant the use of more complex models. Thus, we should not assign too much significance to the values of R_{HS} and τ from our fits. Additional characterization techniques will be necessary to fully quantify the intermicellar potential in these systems.

We find low-q exponents, x, in the range of −2.9 to −3.8. Moreover, as the strength of attraction decreases (f increases), the exponent x systematically decreases, approaching a value of −4. As mentioned above, low q exponents between −3 and −4 are indicative of surface scattering, with the limit of −4 corresponding to smooth interfaces and scattering from rough surfaces yielding exponents closer to −3. Thus, we believe that we have large, compact, polydisperse aggregates with "rough" interfaces. The interfaces between these aggregates and the surroundings become smoother as the strength of attraction is decreased. Similar surface scattering has been observed in polypeptide gels[23] where it arises from the interface of water channels within the gel.

Spectra for different values of f cross one another within the USANS regime, and it appears that the slope increases at lower wavevectors for some samples, most noticeably for f = 0.44 and 0.79. Thus, within a sample, the larger aggregates may be somewhat "smoother", indicating that there may be competing driving mechanisms for formation of large aggregates (e.g., gelation or glass formation versus phase separation).

The fluorescence microscopy photos for f values of 0.44, 0.61, and 0.97 are shown in Figure 3. The bar in the micrographs represents 100 μm. In the images, the brighter regions represent where the BODIPY dye has concentrated. In our case, we assume that the hydrophobic polystyrene would be the most favorable for the dye to partition in. The images show that at low values of f, where the attraction between micelles is greatest, we see the formation of aggregates with length scales of 1−100 μm, confirming the USANS results. As f increases, we see that the number and size of these aggregates appears to diminish.

(18) Crichton, M. A.; Bhatia, S. R. *J. Appl. Polym. Sci.* **2004**, *93*, 490−497.
(19) Vlassopoulus, D.; Fytas, G.; Pispas, S.; Hadjichristis, N. *Physica B* **2001**, *296*, 184−189.
(20) Shusharina, N.; Linse, P.; Khokhlov, A. R. *Macromolecules* **2000**, *10*, 3892−3901.
(21) Zhulina, E. B.; Borisov, O. V. *Macromolecules* **2002**, *35*, 9191−9203.
(22) Crichton, M. A. Ph.D. Thesis, University of Massachusetts, 2005.
(23) Schneider, J. P.; Pochan, D. J.; Ozbas, B.; Rajaopal, K.; Pakstis, L.; Kretsinger, J. *J. Am. Chem. Soc.* **2002**, *124*, 15030−15037.

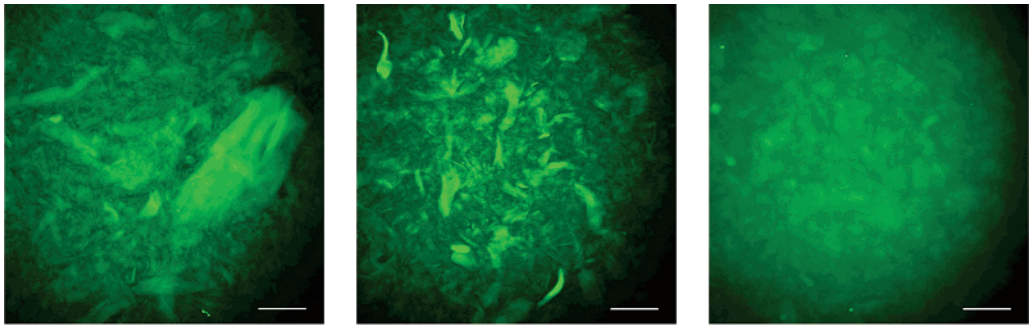

Figure 3. Fluorescence micrograph of 2 wt % PS−PAA/EA gel in water for (a) $f = 0.44$, (b) $f = 0.61$, and (c) $f = 0.97$. Bar represents 100 μm.

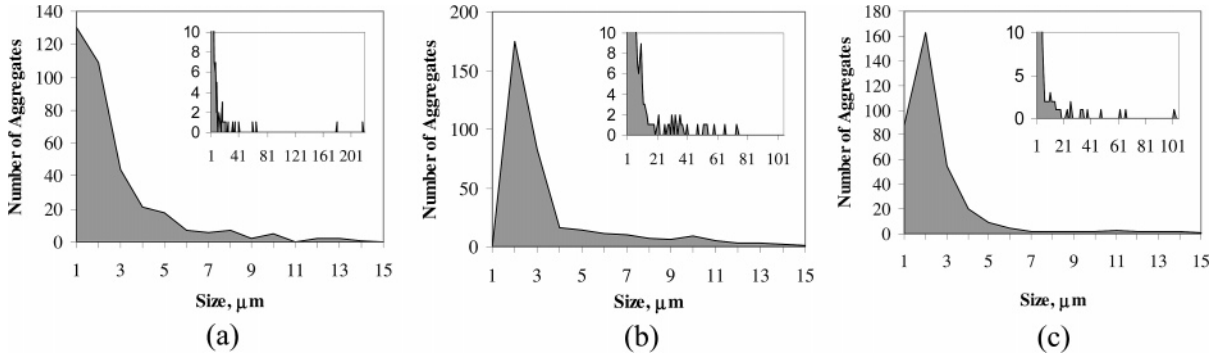

Figure 4. Size distributions from fluorescence micrographs of 2 wt % PS−PAA/EA gel in water for (a) $f = 0.44$, (b) $f = 0.61$, and (c) $f = 0.97$ in the range 1−15 μm. Insets are size distributions over the entire range of aggregate sizes that were calculated.

Table 2. Parameters from Analysis of Microscopy Images

f	average length (μm)	width of distribution (μm)
0.44	38.6	81.8
0.61	21.0	34.8
0.97	23.6	39.7

To quantify this observation, image analysis was performed using several micrographs for each sample. Using ImageJ software, each micrograph was segmented into bright and dark regions. After segmentation, the area of the aggregates was determined, and a distribution of aggregate areas was generated. The characteristic length for the aggregates was taken to be the square root of the area. The resulting aggregate size distributions are shown in Figure 4, and Table 2 gives the average size and width of the distribution. Although the average aggregate sizes are in the range 20−40 μm, the distributions are quite skewed toward smaller diameters (Figure 4). Thus, a more representative measure of the aggregate size is the mode of the distribution, which is 1−2 μm, corresponding to 50−100 micelle diameters. It is likely that some aggregates smaller than 1 μm are present but are not detectable via optical techniques. The aggregates are highly polydisperse as indicated by the large width of the distribution, again confirming our USANS results.

It is possible that the very large structures we observe are the result of phase separation, or a competition between phase separation and gelation or glass formation. It is quite difficult to experimentally determine the role that phase separation plays in this system. We have monitored these samples using fluorescence microscopy over periods of roughly 30 days and not observed growth in the size of aggregates. Fluorescence microscopy over a longer time period is difficult due to photobleaching of the samples. We have not visually observed any macrophase separation in these samples over approximately four years. Finally, our USANS spectra appear quite different than poly(vinyl alcohol) gels undergoing phase separation, which show a broad peak that grows over time.[17] If phase separation is playing a role in the formation of larger aggregates, the dynamics are likely quite slow and difficult to capture experimentally. We are working with collaborators to perform simulations on these systems, which may yield more insight into aggregate formation.

Conclusions

USANS and microscopy shows the existence of large-scale structure in micellar gels of block polyelectrolytes. The low q scattering is not indicative of fractal aggregates; rather, surface scattering is observed from large, polydisperse, dense aggregates with rough interfaces. The interface seems to become smoother as the strength of attraction is decreased, and the low q exponent tends toward −4. Phase separation may be driving formation of some of the very large aggregates in these systems; however, the kinetics of this are too slow to probe experimentally. Further study is needed to determine if similar scattering is observed in attractive glasses of hard colloids and to clarify the role of phase separation versus gel formation in these systems.

Acknowledgment. USANS and SANS data were taken with the assistance of John Barker, Steve Kline, Boualem Hammouda, and Derek Ho at NIST. We thank Prof. Neil S. Forbes, UMass Chemical Engineering, for the use of his fluorescence microscope. This portion of the work utilized facilities supported in part by the National Science Foundation (NSF) under Agreement No. DMR-0086210. We acknowledge the support of the National Institute of Standards and Technology, U.S. Department of Commerce, in providing the neutron research facilities used in this portion of the work. Partial support for M.A.C. was provided by the NSF under Grant CTS-0238873.

LA0508487